

# Distances to Nearby Galaxies in Sculptor <sup>★</sup>

I. D. Karachentsev<sup>1</sup>, E. K. Grebel<sup>2</sup>, M. E. Sharina<sup>1,10</sup>, A. E. Dolphin<sup>3</sup>,  
D. Geisler<sup>4</sup>, P. Guhathakurta<sup>5</sup>, P. W. Hodge<sup>6</sup>, V. E. Karachentseva<sup>7</sup>,  
A. Sarajedini<sup>8</sup>, and P. Seitzer<sup>9</sup>

<sup>1</sup> Special Astrophysical Observatory, Russian Academy of Sciences, N. Arkhyz,  
KChR, 369167, Russia

<sup>2</sup> Max-Planck-Institut für Astronomie, Königstuhl 17, D-69117 Heidelberg,  
Germany

<sup>3</sup> Kitt Peak National Observatory, National Optical Astronomy Observatories,  
P.O. Box 26732, Tucson, AZ 85726, USA

<sup>4</sup> Departamento de Física, Grupo de Astronomía, Universidad de Concepción,  
Casilla 160-C, Concepción, Chile

<sup>5</sup> UCO/Lick Observatory, University of California at Santa Cruz, Santa Cruz,  
CA 95064, USA

<sup>6</sup> Department of Astronomy, University of Washington, Box 351580, Seattle, WA  
98195, USA

<sup>7</sup> Astronomical Observatory of Kiev University, 04053, Observatorna 3, Kiev,  
Ukraine

<sup>8</sup> Department of Astronomy, University of Florida, Gainesville, FL 32611, USA

<sup>9</sup> Department of Astronomy, University of Michigan, 830 Dennison Building,  
Ann Arbor, MI 48109, USA

<sup>10</sup> Isaac Newton Institute, Chile, SAO Branch

Received: December 10, 2002

**Abstract.** We present an analysis of Hubble Space Telescope/WFPC2 images of nine nearby galaxies in Sculptor. We derive their distances from the luminosity of the tip of the red giant branch stars with a typical accuracy of  $\sim 12\%$ . Their distances are 4.21 Mpc (Sc 22), 4.92 Mpc (DDO 226), 3.94 Mpc (NGC 253), 3.40 Mpc (KDG 2), 3.34 Mpc (DDO 6), 3.42 Mpc (ESO 540-030), 4.43 Mpc (ESO 245-05), 4.27 Mpc (UGCA 442), and 3.91 Mpc (NGC 7793). The galaxies are concentrated in several spatially separated loose groups around NGC 300, NGC 253, and NGC 7793. The Sculptor galaxy complex together with the CVn I cloud and the Local Group form a 10 Mpc amorphous filament, apparently driven by the free Hubble flow.

**Key words.** galaxies: dwarf — galaxies: distances — galaxies: kinematics and dynamics — Sculptor group

## 1. Introduction

The association of five bright spiral galaxies in the Sculptor constellation, NGC 55, NGC 247, NGC 253, NGC 300, and NGC 7793, has been considered by many authors as the galaxy group closest to the Local Group (LG), at a distance of  $\sim 2$  Mpc. Over the past decades, a number of dwarf galaxies have been found in this area by van den Bergh (1959: DDO 6, DDO 226), Nilsen (1974: UGCA 438, UGCA 442), and Lauberts (1982: ESO sky survey objects). Special searches for fainter irregular (dIrr) and spheroidal (dSph) dwarf galaxies in the Sculptor group were undertaken by Côté et al. (1997), Karachentseva & Karachentsev (1998, 2000), and Jerjen et al. (1998, 2000). In their paper entitled, “Discovery of numerous dwarf galaxies in the two nearest groups of galaxies”, Côté et al. (1997) reported on the discovery of five new dwarf members of the Sculptor group: Sc 2, Sc 18, Sc 22, Sc 24, and Sc 42. However, based on CCD images of the objects obtained by Whiting et al. (2002) and Tully (2003), we conclude that all of them, except Sc 22, are background galaxies, whose HI velocities were confused with Galactic high velocity clouds in the velocity range from +60 to +160 km s<sup>-1</sup>. Recent HI surveys of the Sculptor region by Staveley-Smith et al. (1998), Barnes et al. (2001), de Blok et al. (2002) have not yet led to the discovery of new dwarf members of the group. Jerjen et al. (1998) measured distances to five dwarf galaxies in Sculptor from fluctuations of their surface brightness and showed that the so-called “Sculptor group” turns out to be a loose filament of galaxies extended along a line of sight over  $\sim 5$  Mpc.

In this paper we present new distance measurements for nine galaxies in the Sculptor region, derived from their tip of the red giant branch (TRGB). Together with earlier published TRGB distances to four other galaxies (Karachentsev et al. 2000, 2002) and the distance to NGC 300 from Cepheids (Freedman et al. 1992), this gives us a basis for a more detailed study of the structure of the Sculptor complex.

## 2. WFPC2 photometry

Images of nine galaxies were obtained with the Wide Field and Planetary Camera (WFPC2) aboard the Hubble Space Telescope (HST) between August 24, 1999 and June 28, 2001 as part of our HST snapshot survey of nearby galaxy candidates (Seitzer et al. 1999; Grebel et al. 2000). The galaxies were observed with 600-second exposures taken in the F606W and F814W filters for each object. Digital Sky Survey (DSS) images

---

\* Based on observations made with the NASA/ESA Hubble Space Telescope. The Space Telescope Science Institute is operated by the Association of Universities for Research in Astronomy, Inc. under NASA contract NAS 5-26555.

of these galaxies are shown in Figure 1 with the HST WFPC2 footprints superimposed. The field size of the red DSS-II images is  $8'$ . Small galaxies were usually centered on the WF3 chip, but for some bright objects the WFPC2 position was shifted towards the galaxy periphery to decrease stellar crowding. The WFPC2 images of the galaxies are presented in the upper panels of Figure 2, where both filters are combined.

For photometric measurements we used the HSTphot stellar photometry package developed by Dolphin (2000a). The package has been optimized for the undersampled conditions present in the WFPC2 to work in crowded fields. After removing cosmic rays, simultaneous photometry was performed on the F606W and F814W frames using *multiphot*, with corrections to an aperture with a radius of  $0''.5$ . Charge-transfer efficiency (CTE) corrections and calibrations were then applied, which are based on the Dolphin (2000b) formulae, producing  $V, I$  photometry for all stars detected in both images. Additionally, stars with a signal-to-noise ratio  $S/N < 3$ ,  $|\chi| > 2.0$ , or  $|\text{sharpness}| > 0.4$  in each exposure were eliminated from the final photometry list. The uncertainty of the photometric zero point is estimated to be within  $0^m05$  (Dolphin 2000b).

### 3. TRGB distances to nine galaxies in Sculptor

The tip of red giant branch (TRGB) method provides an efficient tool to measure galaxy distances. The TRGB distances agree with those given by the Cepheid period-luminosity relation to within 5%. As shown by Lee et al. (1993), the TRGB is relatively independent of age and metallicity. In the  $I$  band the TRGB for low-mass stars is found to be stable within  $\sim 0^m1$  (Salaris & Cassisi 1997; Udalski et al. 2001) for metallicities,  $[\text{Fe}/\text{H}]$ , encompassing the entire range from  $-2.1$  to  $-0.7$  dex found in Galactic globular clusters. According to Da Costa & Armandroff (1990), for metal-poor systems the TRGB is located at  $M_I = -4^m05$ . Ferrarese et al. (2000) calibrated the zero point of the TRGB from galaxies with Cepheid distances and estimated  $M_I = -4^m06 \pm 0^m07(\text{random}) \pm 0.13(\text{systematic})$ . A new TRGB calibration,  $M_I = -4^m04 \pm 0^m12$ , was made by Bellazzini et al. (2001) based on photometry and on the distance estimate from a detached eclipsing binary in the Galactic globular cluster  $\omega$  Centauri. For this paper we use  $M_I = -4^m05$ . The lower left panels of Figure 2 show  $I, (V - I)$  color-magnitude diagrams (CMDs) for the nine observed galaxies.

We determined the TRGB using a Gaussian-smoothed  $I$ -band luminosity function (LF) for red stars with colors  $V - I$  within  $\pm 0^m5$  of the mean  $\langle V - I \rangle$  expected for red giant branch stars. Following Sakai et al. (1996), we applied a Sobel edge-detection filter. The position of the TRGB was identified with the peak in the filter response function. The resulting LFs and the Sobel-filtered LFs are shown in the lower right corners of Figure 2. The results are summarized in Table 1. There we list: (1) galaxy name; (2) equatorial coordinates of the galaxy center; (3) galaxy major diameter and axial ratio;

(4) apparent integrated blue magnitude from the NASA Extragalactic Database (NED) and Galactic extinction in the  $B$ -band from Schlegel et al. 1998; (5) morphological type in de Vaucouleurs' notation; (6) heliocentric radial velocity and radial velocity with respect to the LG centroid (Karachentsev & Makarov 1996); (7) position of the TRGB and its uncertainty as derived with the Sobel filter; (8) true distance modulus with its uncertainty, which takes into account the uncertainty in the TRGB, as well as uncertainties of the HST photometry zero point ( $\sim 0^m05$ ), the aperture corrections ( $\sim 0^m05$ ), and the crowding effects ( $\sim 0^m06$ ) added quadratically; the uncertainties in the extinction and reddening are taken to be 10% of their values from Schlegel et al. (1998); [for more details on the total budget of internal and external systematic errors for the TRGB method see Mendez et al. (2002)]; and (9) linear distance in Mpc and its uncertainty.

Given the distance moduli of the galaxies, we can estimate their mean metallicity from the mean color of the TRGB measured at an absolute magnitude  $M_T = -3.5$ , as recommended by Da Costa & Armandroff (1990). Based on a Gaussian fit to the color distribution of the giant stars in a corresponding  $I$ -magnitude interval ( $-3.5 \pm 0.3$ ), we derived their mean colors,  $(V-I)_{-3.5}$ , which lie in the range of 1.18 mag to 1.54 mag after correction for Galactic reddening. Following the relation of Lee et al. (1993), this provides us with mean metallicities  $-1.1 \text{ dex} > \langle [\text{Fe}/\text{H}] \rangle > -2.4 \text{ dex}$ , listed in the last column of Table 1. With a typical statistical scatter of the mean color ( $\sim 0^m05$ ), and uncertainties of the HST photometry zero point we expect the uncertainty in metallicity to be about 0.3 dex. Therefore within the measurement accuracy the metallicity of the galaxies satisfy the required limitation,  $[\text{Fe}/\text{H}] < -0.7 \text{ dex}$ . Below, some individual properties of the galaxies are briefly discussed.

*Sc 22.* This dwarf spheroidal galaxy of very low surface brightness was discovered by Côté et al. (1997). Surface photometry of Sc 22 was carried out by Jerjen et al. (1998, 2000), who determined its integrated apparent magnitude,  $B_T = 17.73 \text{ mag}$ , integrated color,  $(B-R)_T = 0.79 \text{ mag}$ , and central surface brightness,  $25.8^m/\square''$  in the B band. Using the method of surface brightness fluctuations (SBF), they estimated the distance to Sc 22 to be  $2.67 \pm 0.16 \text{ Mpc}$ . The galaxy was not detected in the H I line by Côté et al. (1997), neither was it detected in the “blind” HIPASS survey by Staveley-Smith et al. (1998) and Barnes et al. (2001). The color-magnitude diagram of Sc 22 (see Fig. 2) is populated predominantly by red stars. The application of the Sobel filter yields  $I(\text{TRGB}) = 24^m10 \pm 0^m21$ , which corresponds to a linear distance of  $4.21 \pm 0.43 \text{ Mpc}$ . This is much larger than the SBF distance.

*DDO 226 = IC 1574 = UGCA 9.* This dIrr galaxy has a relatively high radial velocity,  $V_{LG} = 408 \text{ km s}^{-1}$ . The CMD of DDO 226 shows blue and red stellar populations. There is no strong discontinuity in the luminosity function but there is only a slight hint of a red giant branch. Two peaks are seen in the Sobel-filtered luminosity function. The first lower peak at  $I = 23.8$  appears to be caused by AGB stars, and the second one, at

$I = 24^m44 \pm 0^m24$ , which we interpret as the TRGB, yields a linear distance of  $4.92 \pm 0.58$  Mpc.

*NGC 253.* NGC 253 is the brightest galaxy in the Sculptor group. With a size of  $27' \times 6'$ , NGC 253 extends far beyond the WFPC2 field. Surprisingly, this prominent Sc galaxy has so far no reliable distance estimate, apart from a rough estimate of  $D = 2.77$  Mpc derived by Puche & Carignan (1988) from the Tully-Fisher relation. In our HST observations the WFPC2 was pointed to the NE quadrant of the galaxy, where the stellar crowding is lower. The HST photometry measured a total of about 27000, mostly red, stars. The TRGB is located at  $I = 23^m97 \pm 0^m19$ , corresponding to a distance of  $3.94 \pm 0.37$  Mpc. With this distance, the resulting absolute integrated magnitude of NGC 253,  $M_B = -20.14$  mag, turns out to be comparable with the absolute magnitudes of the Milky Way. Like the Milky Way, NGC 253 has a rotation velocity  $V_{max}$  about 225  $\text{km s}^{-1}$ .

*KDG 2 = ESO 540-030 = KK 09.* This dSph galaxy of low surface brightness was found by Karachentseva (1968) and then selected as the Local Volume member candidate by Karachentseva & Karachentsev (1998). According to the surface photometry carried out by Jerjen et al. (1998, 2000), KDG 2 has an integrated magnitude of  $B_T = 16.37$  mag, an integrated color of  $(B - R)_T = 0.83$  mag, and a central surface brightness of  $24.1^m/\square''$  in the  $B$ -band. Jerjen et al. (1998) determined its distance via SBF to be  $3.19 \pm 0.13$  Mpc. The HST photometry measured about 1900 predominantly red stars. We derived the TRGB to be located at  $23^m65 \pm 0^m20$ , which corresponds to  $D = 3.40 \pm 0.34$  Mpc, in good agreement with the previous estimate. Apart from red stars, we also found a number of blue stars, which occupy the central part of the galaxy. Probably, KDG 2 is not a dSph galaxy, but belongs to a transition dSph/dIrr type, like LGS-3 and Antlia. Huchtmeier et al. (2000) did not detect it in the HI line.

*DDO 6 = UGCA 15 = ESO 540-031.* This dIrr galaxy of drop-like shape has a radial velocity of  $V_{LG} = 348 \text{ km s}^{-1}$ . In Fig.2 the CMD shows the presence of mixed blue and red populations, in particular, a prominent population of RGB stars. We determined  $I(\text{TRGB})$  to be  $23^m62 \pm 0^m16$ , yielding  $D = 3.34 \pm 0.24$  Mpc.

*ESO 540-032 = FG 24 = KK 10.* Like KDG 2, FG 24 (Feitzinger & Galinski 1985) has a reddish color and a low surface brightness, typical of dSph or dSph/dIrr galaxies. The galaxy was not detected in HI by Huchtmeier et al. (2000). Surface photometry of FG 24, performed by Jerjen et al. (1998, 2000), yields an integrated magnitude of  $B_T = 16.44$  mag, an integrated color  $(B - R)_T = 1.08$  mag, and a central surface brightness  $24.5^m/\square''$  in the  $B$ -band. Most of the stars detected by us in FG 24 (see Fig. 2) are likely RGB stars, although some faint blue stars are present in the galaxy's central part. The TRGB  $I$ -band magnitude derived by us,  $23^m67 \pm 0^m17$ , corresponds to a distance of  $3.42 \pm 0.27$  Mpc, which exceeds the distance  $2.21 \pm 0.14$  Mpc estimated by Jerjen et al.

(1998) from SBF, but agrees excellently with the new distance estimate,  $3.4 \pm 0.2$  Mpc, obtained by Jerjen & Rejkuba (2001) from the TRGB.

*ESO 245-005*. This irregular galaxy of Magellanic type has an angular dimension of  $3'8 \times 3'4$  and a radial velocity of  $V_{LG} = 308 \text{ km s}^{-1}$ . In the WFPC2 image of its central bar-like part we detected about 11000 blue and red stars. We determined the *I*-band TRGB to be at  $24^m22 \pm 0^m21$ , yielding a distance of  $4.43 \pm 0.45$  Mpc.

*UGCA 442 = ESO 471-06*. This is an edge-on galaxy of Im type with a radial velocity  $V_{LG} = 299 \text{ km s}^{-1}$  and angular dimension  $6'4 \times 0'9$ , much larger than the WFPC2 field. The galaxy seems to be well resolved into stars. Our HST photometry reveals about 5600 stars, both blue and red ones. The derived TRGB,  $I = 24^m13 \pm 0^m26$ , corresponds to a distance of  $4.27 \pm 0.52$  Mpc.

*NGC 7793*. This is a bright spiral galaxy with a dimension of  $9'3 \times 6'3$  and with a radial velocity  $V_{LG} = 252 \text{ km s}^{-1}$ . The WFPC2 was pointed at its eastern side. We obtained photometry for about 22000 stars. The CMD shows a mixture of young and old stellar populations. The TRGB magnitude,  $23^m95 \pm 0^m22$ , yields a galaxy distance of  $3.91 \pm 0.41$  Mpc, in reasonable agreement with the distance  $3.27 \pm 0.08$  Mpc derived by Puche & Carignan (1988) from the Tully-Fisher relation.

#### 4. Structure and kinematics of the Sculptor group

To study the 3-D structure of the Sculptor complex, we collected the most complete sample of data on all known nearby galaxies situated in this region of the sky. Table 2 presents the following characteristics of the 21 galaxies in our sample: (1) galaxy name; (2) equatorial (upper line), and Supergalactic (lower line) coordinates; (3) major angular diameter in arcmin and apparent axial ratio; (4) apparent integrated magnitude from NED and Galactic extinction from Schlegel et al. (1998) in the B-band; (5) morphological type; (6) heliocentric radial velocity in  $\text{km s}^{-1}$  and velocity in the Local Group rest frame (Karachentsev & Makarov 1996); (7) the H I line width (in  $\text{km s}^{-1}$ ) at the 50% level of the maximum from LEDA (Paturel et al. 1996) or HIPASS, corrected for galaxy inclination (upper line), and absolute magnitude of the galaxy, corrected for Galactic extinction (lower line); (8) distance to the galaxy in Mpc from the Milky Way (upper line), and from the Local Group centroid (lower line), respectively. The last column gives the method used for distance measurement (“Cep” — from Cepheids, “RGB” — from TRGB, “SBF” — from surface brightness fluctuations, and “TF” — from the Tully-Fisher relation), and the distance data reference.

Apart from four dSph galaxies with known distances but unknown radial velocities (KK 3, Sc 22, KDG 2, and FG 24), we also included in Table 2 the low surface brightness galaxy KK 258, which looks like a nearby semi-resolved system in a CCD image obtained by Whiting et al. (2002). Its distance and velocity are both unknown. In comparison

with the TRGB distances, the distance estimates of Sc 22, KDG 2 and FG 24 from SBF (Jerjen et al. 1998) are systematically lower on 0.9 Mpc, which is why we increased their original SBF distance estimate for NGC 59 from 4.4 Mpc to 5.3 Mpc.

The distribution of the 21 galaxies from Table 2 is presented in Fig. 3 in equatorial coordinates. Three of the brightest spiral galaxies are shown as filled squares, and dIrr and dSph galaxies are shown as filled and open circles, respectively. Radial velocities of the galaxies with respect to the LG centroid are indicated by numbers. As can be seen, the distribution of galaxies in Sculptor does not exhibit any distinct center, and it does not show a sharp boundary either. Most of the galaxies are situated at low supergalactic latitudes,  $|\text{SGB}| < 10^\circ$ , where projection effects makes it difficult to restore the 3-D structure of the group. Referring to Table 3, we recognize that the spiral galaxy NGC 253 surpasses all other galaxies in this group by more than a factor of five in luminosity. Therefore, we consider NGC 253 as the dynamical center of the Sculptor group.

Puche & Carignan (1988) estimated the distance to NGC 253 and some other galaxies in Sculptor, based on the Tully-Fisher relation. However, for their calibration, they used old data on galaxy distances. A revised relation “absolute magnitude — H I line width” for 6 galaxies in Sculptor with new distance estimates is presented in Fig. 4. Here, the line width is corrected for galaxy inclination to the line of sight. Using the regression line,  $M_B = -7.0 \log(W_c) - 1.8$ , we estimated the distances to five galaxies: NGC 55, NGC 247, NGC 625, ESO 349–031, and ESO 149–03, presented in column (8) of Table 2.

The Hubble diagram showing velocity versus distance for 20 galaxies in Sculptor is given in Fig. 5. Galaxies with accurate distance estimates (“Cep”, “RGB”, “SBF”) are shown as filled circles, while galaxies with distances from the T-F relation are indicated by crosses, and the brightest spiral galaxy NGC 253 is shown as a square. Four dSph galaxies without velocities are shown conditionally by vertical bars. The solid curve corresponds to the Hubble parameter  $H = 75 \text{ km s}^{-1} \text{ Mpc}^{-1}$ . At small distances this curve deviates from a straight line due to a decelerating gravitational action of the Local Group, the total mass of which is adopted to be  $M_{LG} = 1.3 \cdot 10^{12} \cdot M_\odot$  (Karachentsev et al. 2002).

Based on the data in Fig. 3 and Fig. 5, we can describe the structure of the galaxy complex in Sculptor in the following way.

a) Three galaxies with  $V_{LG} > 400 \text{ km s}^{-1}$  (ESO 149–03, NGC 59, and DDO 226) apparently are background objects. NGC 59 and DDO 226 probably form a wide pair with a linear projected distance of 580 kpc and a radial velocity difference of  $13 \text{ km s}^{-1}$ .

b) In front of the complex there is a pair of bright galaxies, NGC 300 and NGC 55, with two dSph companions, ESO 410–05 and ESO 294–10. The mean distance to this loose quartet is 1.95 Mpc. This is only 0.6 Mpc more distant than to another known loose quartet: NGC 3109, Sex A, Sex B, and Antlia, located at the LG edge. Possibly,

two other dIrr galaxies, UGCA 438 and IC 5152, are associated with the NGC 300 group, too.

c) The brightest spiral galaxy NGC 253 together with its companions, NGC 247, DDO 6, Sc 22, KDG 2 and FG 24, can be considered as the Sculptor complex' core. The last three dSph galaxies do not have radial velocities so far. Apart from the NGC 253 group, there is a galaxy triplet, NGC 7793, UGCA 442, and ESO 349–031. The line of sight distances to NGC 253 and NGC 7793 are almost the same within the measurement errors.

d) Among the remaining galaxies, NGC 625 and ESO 245–05 have an angular separation of  $2^{\circ}9$  and a radial velocity difference of only  $27 \text{ km s}^{-1}$ . However, their distance estimates differ significantly. Because NGC 625 deviates essentially from the Hubble regression line in Fig. 5, we assume its T-F distance to be underestimated by approximately 2 Mpc. This assumption can be easily proven by measuring the TRGB distance to this poorly studied galaxy.

The total mass of each group can be estimated from the virial balance of kinetic and potential energies (Limber & Mathews 1960),

$$M_{vir} = 3\pi N \cdot (N - 1)^{-1} \cdot G^{-1} \cdot \sigma_v^2 \cdot R_H, \quad (1)$$

where  $N$  is the number of galaxies in the group,  $\sigma_v^2$  is the radial velocity dispersion,  $R_H$  is the mean projected harmonic radius, and  $G$  is the gravitational constant. Such an approach assumes that the characteristic crossing time of the group,  $T_{cross} = \langle R_p \rangle / \sigma_v$ , is low in comparison with the age of the Universe (here  $\langle R_p \rangle$  means the average projected radius of the group).

Another way to estimate the total mass of a group was proposed by Bahcall & Tremaine (1981). Assuming the motions of dwarf galaxies around the main group member to be closed Keplerian motions with orbit eccentricity  $e$ , in the case of random orientation of galaxy orbits we obtain

$$M_{orb} = (32/3\pi) \cdot G^{-1} \cdot (1 - 2e^2/3)^{-1} \langle R_p \cdot \Delta V_r^2 \rangle, \quad (2)$$

where  $R_p$  and  $\Delta V$  are projected distance and radial velocity of a companion with respect to the main group member.

The basic dynamical parameters of the three mentioned groups in Sculptor are presented in Table 3. In the case of orbital mass estimates the mean eccentricity  $e = 0.7$  is adopted. As seen from these data, the virial/orbital mass-to-luminosity ratios of the groups lie in the range of 45 to  $260 M_{\odot}/L_{\odot}$ . However, for all the groups their crossing time, 6 – 18 Gyr, is comparable to the time of cosmic expansion,  $1/H_0$ , which makes the derived mass estimates very unreliable.

According to Lynden-Bell (1981) and Sandage (1986), in the expanding universe any dense enough group with a total mass  $M_0$  may be characterized by a “zero-velocity surface”, which separates the group from the Hubble flow. In the case of spherical symmetry,



the radius of this surface,  $R_0$ , is expressed via the total mass of the group and the Hubble constant,  $H_0$ , by a simple relation

$$M_0 = (\pi^2/8G) \cdot H_0^2 \cdot R_0^3. \quad (3)$$

For estimating  $R_0$ , we calculated for any galaxy with the distance  $D$  and radial velocity  $V$  its spatial separation from NGC 253

$$R^2 = D^2 + D_{N253}^2 - 2D \cdot D_{N253} \cdot \cos \theta$$

and its projected radial velocity with respect to NGC 253

$$(V - V_{N253})_p = V \cdot \cos \lambda - V_{N253} \cdot \cos(\theta + \lambda),$$

where  $\theta$  is an angular distance of the galaxy from NGC 253, and  $\tan \lambda = D_{N253} \cdot \sin \theta / (D - D_{N253} \cdot \cos \theta)$ . Here we assumed that the peculiar velocities of the galaxies are small in comparison with velocities of the regular Hubble flow. The estimated values  $(V - V_{N253})_p$  and  $R$  for 15 galaxies around NGC 253 are presented in column (9) of Table 2. The distribution of relative radial velocities and spatial separations is shown in Fig. 6. Here galaxies with accurate (“Cep”, “RGB”, “SBF”) and with rough (“TF”) distance estimates are indicated by filled circles and crosses, respectively. As seen from Fig. 6, among sufficiently distant galaxies with  $R > 0.7 \text{ Mpc}$  there are no galaxies approaching NGC 253 (the region of cosmological expansion). In particular, NGC 7793 together with its companions move away from NGC 253 too. But within  $R < 0.7 \text{ Mpc}$  there are galaxies both with negative (DDO 6) as well as positive (NGC 247) velocities with respect to NGC 253 (“virialized” zone). Based on these (still incomplete) data we can conclude that the radius of the zero-velocity surface for the NGC 253 group is  $R_0 = 0.7 \pm 0.1 \text{ Mpc}$ . According to equation (3) this corresponds to a total mass of  $M_0 = (0.55 \pm 0.22) 10^{12} M_\odot$  or  $M_0/L_B = (29 \pm 11) M_\odot/L_\odot$ , which is 3–5 times lower than the virial/orbital mass estimates derived above. Measurements of radial velocities for the remaining four dSph galaxies, situated in the range  $R = 0.47 - 2.07 \text{ Mpc}$ , will allow one to derive the radius  $R_0$  and the total mass of the NGC 253 group with higher accuracy.

## 5. Concluding remarks

Our measurements of accurate distances to 9 galaxies in Sculptor clarified the structure and kinematics of this nearby complex of galaxies. However, nine other presumably nearby galaxies in the same area (with  $V_{LG} < 500 \text{ km s}^{-1}$  or  $D < 5 \text{ Mpc}$ ) still remain without reliable distance estimates (NGC 55, NGC 625, NGC 247, SDIG, and ESO 149-03) or radial velocity estimates (ESO 410-05, KDG 2, FG 24, and Sc 22). Our new data on galaxy distances confirm the conclusion drawn by Jerjen et al. (1998) that the so-called group in Sculptor is a loose “cloud” of galaxies of  $1 \times 6 \text{ Mpc}$  in size, extended along the

line of sight. Apparently, the near and the far parts of this “cigar” are not gravitationally bound to each other, but take part in the general Hubble flow. In this sense, the Sculptor cloud looks like another nearby cloud, Canes Venatici I (Karachentsev et al. 2003). Both these loose clouds are populated mostly by dwarf galaxies, and their luminosity function has a flat “primordial” shape. As was noted by Jerjen et al.(1998) and Karachentsev et al.(2003), the galaxy complexes in Sculptor and Canes Venatici together with the Local Group form an amorphous filament extending over  $\sim 10$  Mpc.

The nearby galaxy complex in Sculptor is a suitable case to study the “anatomy” of virial mass excess. In projection onto the sky, the Sculptor filament has a rather high overdensity, and can be easily identified as a usual group by the “friend of friends” algorithm (Huchra & Geller 1982) or by the method of hierarchical trees (Materne 1978). In his Nearby Galaxy Catalog, Tully (1988) denotes the Sculptor group by the number “14–13”. Based on radial velocities and projected separations of 11 members of the group, Tully (1987) estimated its virial mass-to-luminosity ratio to be  $M_{vir}/L_B = 328M_{\odot}/L_{\odot}$ . There the galaxies NGC 55, NGC 253, NGC 7793, and DDO 226 were considered as members of a single group. Apart from real and probable members of the Sculptor complex, Tully included in the group also the galaxy PGC 71145, whose radial velocity is  $+16 \text{ km s}^{-1}$  (instead of  $+1600 \text{ km s}^{-1}$  as a result of a misprint in Longmore et al. 1982). Comparing the ratio  $M_{vir}/L_B$  from Tully (1987) with our estimate of the total mass-to-luminosity ratio,  $29 \pm 11 M_{\odot}/L_{\odot}$ , we conclude that by using the more reliable and precise observational data that are now available, as well as our new approach to the determination of mass, can decrease the total mass estimate of the group by one order of magnitude.

*Acknowledgements.* The authors wish to thank C.Carignan, the referee, for his useful comments. Support for this work was provided by NASA through grant GO–08601.01– A from the Space Telescope Science Institute, which is operated by the Association of Universities for Research in Astronomy, Inc., under NASA contract NAS5–26555. This work was partially supported by RFBR grant 01–02–16001 and DFG-RFBR grant 02–02–04012. D.G. gratefully acknowledges support from the Chile *Centro de Astrofísica* FONDAF No. 15010003.

The Digitized Sky Surveys were produced at the Space Telescope Science Institute under U.S. Government grant NAG W–2166. The images of these surveys are based on photographic data obtained using the Oschin Schmidt Telescope on the Palomar Mountain and the UK Schmidt Telescope. The plates were processed into the present compressed digital form with permission of these institutions.

This project made use of the NASA/IPAC Extragalactic Database (NED), which is operated by the Jet Propulsion Laboratory, Caltech, under contract with the National Aeronautics and Space Administration.

## References

Bahcall J.N., Tremaine S., 1981, ApJ 244, 805

- Barnes D.G., Staveley-Smith L., de Blok W.J., 2001, MNRAS 322, 486
- Côte S., Freeman K.C., Carignan C., Quinn P.J., 1997, AJ 114, 1313
- Bellazzini M., Ferraro F.R., Pancino E., 2001, ApJ 556, 635
- Da Costa G.S., Armandroff T.E., 1990, AJ 100, 162
- de Blok W.J., Zwaan M.A., Dijkstra M., et al, 2002, (a-ph/0111238)
- Dolphin A.E., 2000a, PASP 112, 1383
- Dolphin A.E., 2000b, PASP 112, 1397
- Feitzinger J.W., Galinski T., 1985, A&AS 61, 503
- Ferrarese L., et al. 2000, ApJ 529, 745
- Freedman W., Madore B.F., Hawley S.L., et al, 1992, ApJ 396, 80
- Grebel E.K., et al. 2000, in “Stars, Gas, and Dust in Galaxies: Exploring the Links,” ASP Conf. Ser. 221, eds. D. Alloin, K. Olsen (Provo: ASP), 147
- Huchra J.P., Geller M.J., 1982, ApJ 257, 423
- Huchtmeier W.K., Karachentsev I.D., Karachentseva V.E., Ehle M., 2000, A&AS 141, 469
- Jerjen H., Rejkuba M., 2001, A&A 371, 487
- Jerjen H., Freeman K.C., Binggeli B., 2000, AJ 119, 166
- Jerjen H., Freeman K.C., Binggeli B., 1998, AJ 116, 2873
- Karachentsev I.D., Makarov D.I., Sharina M.E., et al, 2003, A&A, 398, 467
- Karachentsev I.D., Sharina M.E., Makarov D.I., et al, 2002 A&A 389, 812
- Karachentsev I.D., Sharina M.E., Grebel E.K., et al, 2000, ApJ 542, 128
- Karachentsev I., Makarov D., 1996, AJ 111, 535
- Karachentseva V.E., Karachentsev I.D., 2000, A&AS 146, 359
- Karachentseva V.E., Karachentsev I.D., 1998, A&AS 127, 409
- Lauberts A., 1982, ESO/Uppsala Survey of ESO(B) Atlas, Garching, ESO
- Lee M.G., Freedman W.L. Madore B.F., 1993, ApJ 417, 553
- Limber D.N., Mathews W.G., 1960, ApJ 132, 286
- Longmore A.J., Hawarden T.G., Mebold U., et al, 1982, MNRAS 200, 325
- Lynden-Bell D., 1981, Observatory 101, 111
- Materne J., 1978, A&A 63, 401
- Mendez B., Davis M., Moustakas J., et al., 2002, AJ 124, 213
- Nilsen P., 1974, Uppsala Astr. Observ. report 5, 1
- Paturel G., Bottinelli L., Di Nella H. et al, 1996, Catalogue of Principal Galaxies, (LEDA),  
Saint-Genis Laval, Observatoire de Lyon
- Puche D., Carignan C., 1988, AJ 95, 1025
- Sakai S., Madore B.F., 1999, ApJ 526, 599
- Sakai S., Madore B.F., Freedman W.L., 1996, ApJ 461, 713
- Salaris M., Cassisi S., 1997, MNRAS 289, 406
- Sandage A., 1986, ApJ 307, 1
- Schlegel D.J., Finkbeiner D.P., Davis M., 1998, ApJ 500, 525
- Seitzer P., Grebel E.K., Dolphin A.E., et al, 1999, BAAS
- Staveley-Smith L., Yuraszek S., Koribalski B.S., et al, 1998, AJ 116, 2717
- Tully R.B., 1987, ApJ, 321, 280
- Tully R.B., 1988, Nearby Galaxy Catalog, Cambridge Univ. Press

**Table 1.** New distances to galaxies in Sculptor region.

Name	RA (B1950) Dec	$a$ $b/a$	$B_T$ $A_b$	$T$	$V_h$ $V_{LG}$	$I(TRGB)$	$(m - M)_0$	$D_{MW}$	$(V - I)_{-3.5}$ [Fe/H]
Sc22	002121.0–245855	0.9	17.73	–3		24.10	28.12	4.21	1.40
		.78	0.06			0.21	0.23	0.43	–1.51
DDO226	004035.0–223127	2.2	14.36	10	357	24.44	28.46	4.92	1.28
		.36	0.07		408	0.24	0.26	0.58	–1.96
N253	004506.9–253354	26.7	7.92	5	241	23.97	27.98	3.94	1.54
		.22	0.08		274	0.19	0.21	0.37	–1.12
KDG2 E540–030	004651.9–182048	1.2	16.37	–1		23.65	27.66	3.40	1.37
		.92	0.10			0.20	0.22	0.34	–1.61
DDO6	004721.0–211718	1.7	15.19	10	295	23.60	27.62	3.34	1.25
		.41	0.07		348	0.13	0.16	0.24	–2.08
E540–032 FG24	004756.0–201044	1.3	16.44	–3		23.66	27.67	3.42	1.42
		.92	0.09			0.14	0.17	0.27	–1.45
E245–05 P6430	014257.9–435054	3.8	12.73	10	394	24.22	28.23	4.43	1.25
		0.89	0.07		308	0.21	0.23	0.45	–2.08
UA442	234109.0–321412	6.4	13.58	9	267	24.13	28.15	4.27	1.18
		.14	0.07		299	0.26	0.27	0.52	–2.40
N7793	235515.0–325206	9.3	9.70	7	229	23.95	27.96	3.91	1.50
		.68	0.08		252	0.22	0.24	0.41	–1.22

Tully R.B., 2003, private communication

Udalski A., Wyrzykowski L., Pietrzynski G., et al, 2001, Acta Astronomica 51, 221

van den Bergh S., 1959, Publ. David Dunlap Obs., II, No 5

Whiting A.B., Hau G.K., Irwin M., 2002, ApJS 141, 123

**Table 2.** List of 21 nearby galaxies in the Sculptor group region.

Name	RA (B1950) Dec		$a$	$B_T$	$T$	$V_h$	$W_{50}^c$	$D_{MW}$	$dV_p$	Notes
	$SGL$	$SGB$	$b/a$	$A_b$		$V_{LG}$	$M_b$	$D_{LG}$	$R$	
E349-031	000540.9-345124		1.1	15.48	10	207	35	4.1	44	TF
SDIG	260.18+0.40		.82	0.05		216	-12.65	4.02	0.90	present paper
N55	001238.0-392954		32.4	8.84	9	129	175	1.8	170	TF
	256.25-2.36		.17	0.06		111	-17.50	1.78	2.26	present paper
N59	001253.0-214318		2.7	13.12	-3	361		5.3	164	SBF
KK2	273.13+3.15		.48	0.09		431	-15.59	5.12	1.62	Jerjen &, 1998
E410-005	001300.3-322728		1.3	14.90	-1			1.92		RGB
KK3	262.95-0.26		.77	0.06			-11.58	1.85		Kar. &,2000
Sc22	002121.0-245855		0.9	17.73	-3			4.21		RGB
	270.62+0.31		.78	0.06			-10.45	4.05		present paper
E294-010	002406.2-420756		1.1	15.60	-3	117		1.92	195	RGB
	254.37-5.27		.64	0.02		81	-10.84	1.85	2.06	Kar. &,2002
DDO226	004035.0-223127		2.2	14.36	10	357	51	4.92	134	RGB
	274.23-3.21		.36	0.07		408	-14.17	4.74	1.01	present paper
N247	004439.6-210158		21.4	9.86	7	160	222	4.09	19	TF
	275.92-3.73		.32	0.08		215	-18.28	3.90	0.36	present paper
N253	004506.9-253354		26.7	7.92	5	241	420	3.94	0	RGB
	271.57-5.01		.22	0.08		274	-20.14	3.79	0	present paper
KDG2	004651.9-182048		1.2	16.37	-1			3.40		RGB
E540-030	278.65-3.52		.92	0.10			-11.39	3.20		present paper
DDO6	004721.0-211718		1.7	15.19	10	295	24	3.34	-53	RGB
	275.84-4.40		.41	0.07		348	-12.50	3.16	0.55	present paper
E540-032	004756.0-201044		1.3	16.44	-3			3.42		RGB
FG24	276.95-4.24		.92	0.09			-11.32	3.23		present paper
N300	005231.8-375712		21.9	8.95	7	144	212	2.15	163	Cep
	259.81-9.50		.71	0.06		114	-17.77	2.11	1.78	Freedman &,1992

N625	013254.9–414130	6.4	11.59	9	405	94	2.7:	23	TF
	257.26–17.74	.28	0.07		335	–15.64	2.69	1.65:	present paper
E245–05	014257.9–435054	3.8	12.73	9	394		4.43	116	RGB
	255.14–19.74	.89	0.07		308	–15.57	4.30	1.67	present paper
I5152	215926.6–513214	5.2	11.06	10	124	116	2.07	212	RGB
E237–27	234.23+11.53	.62	0.11		75	–15.63	2.18	2.63	Kar. &, 2002
KK258	223756.3–310340	1.6	17.36	–3					
	255.48+18.58	.50	0.06						
UA438	232347.3–323957	1.5	13.86	10	62	57	2.23	179	RGB
	258.88+9.28	.80	0.06		99	–12.94	2.16	1.86	Kar. &, 2002
UA442	234109.0–321412	6.4	13.58	9	267	94	4.27	82	RGB
	260.78+6.12	.14	0.07		299	–14.64	4.01	1.15	present paper
E149–003	234925.5–525121	2.2	15.0	10	577	56	6.4	293	TF
	242.31–3.23	.18	0.06		501	–14.10	6.44	3.54	present paper
N7793	235515.0–325206	9.3	9.70	7	229	237	3.91	60	RGB
	261.30+3.12	.68	0.08		252	–18.34	3.82	0.90	present paper

**Table 3.** Properties of nearby groups in Sculptor.

Group	$N$	$D$ Mpc	$\langle R_p \rangle$ kpc	$\sigma_V$ km s <sup>–1</sup>	$L_B$ 10 <sup>10</sup> $L_\odot$	$M_{vir}/L_B$ $M_\odot/L_\odot$	$M_{orb}/L_B$ $M_\odot/L_\odot$	$T_{cross}$ Gyr
N300, N55, E294–10, E410–05	4	1.95	279	15	0.33	54	45	18.6
N253, N247, DDO6, Sc22, KDG2, FG24	6	3.94	370	54	1.91	143	83	6.9
N7793, UA442, E349–31	3	3.91	205	34	0.30	260	140	6.0

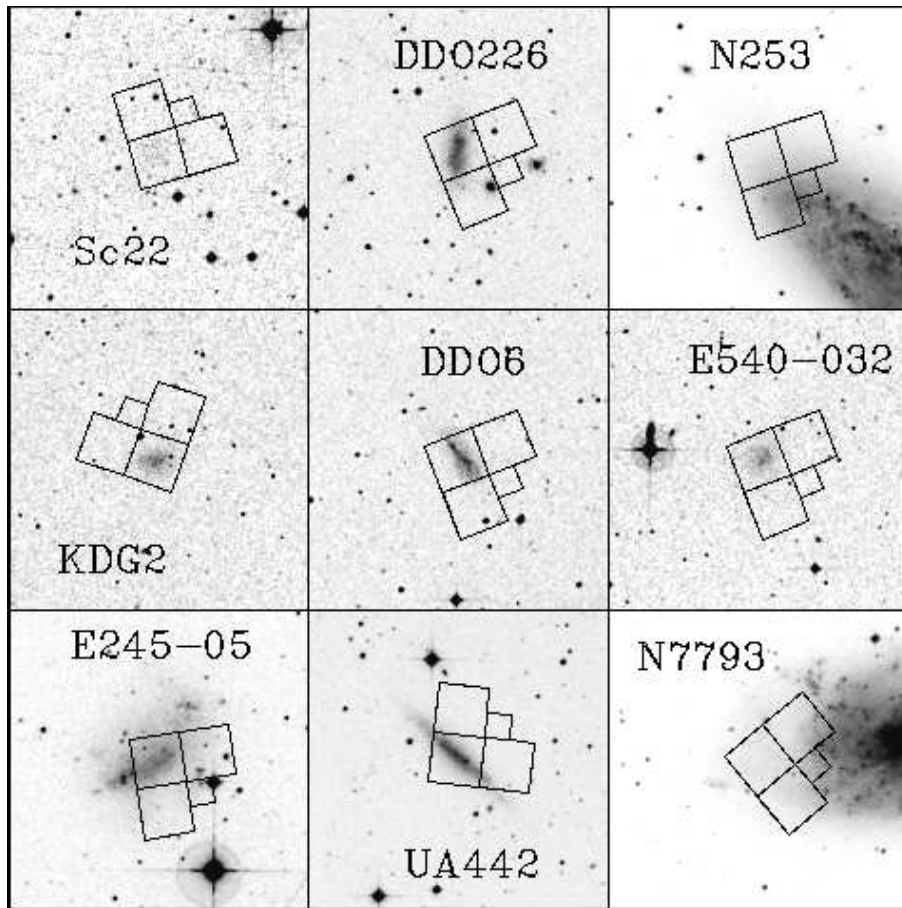


**Fig. 1.** Digital Sky Survey images of 9 nearby galaxies in Sculptor. The field size is  $8'$ , North is up and East is left. The HST WFPC2 footprints are superimposed.

**Fig. 2. Top:** WFPC2 images of nine galaxies: Sc 22, DDO 226, NGC 253, KDG 2, DDO 6, ESO 540–032, ESO 245–05, UGCA 442, and NGC 7793 produced by combining the two 600s exposures obtained through the F606W and F814W filters. The arrows point to the North and the East. **Bottom left:** The color-magnitude diagrams from the WFPC2 data for the nine galaxies in Sculptor. **Bottom right:** The Gaussian-smoothed *I*-band luminosity function restricted to red stars (top), and the output of an edge-detection filter applied to the luminosity function for the nine galaxies.

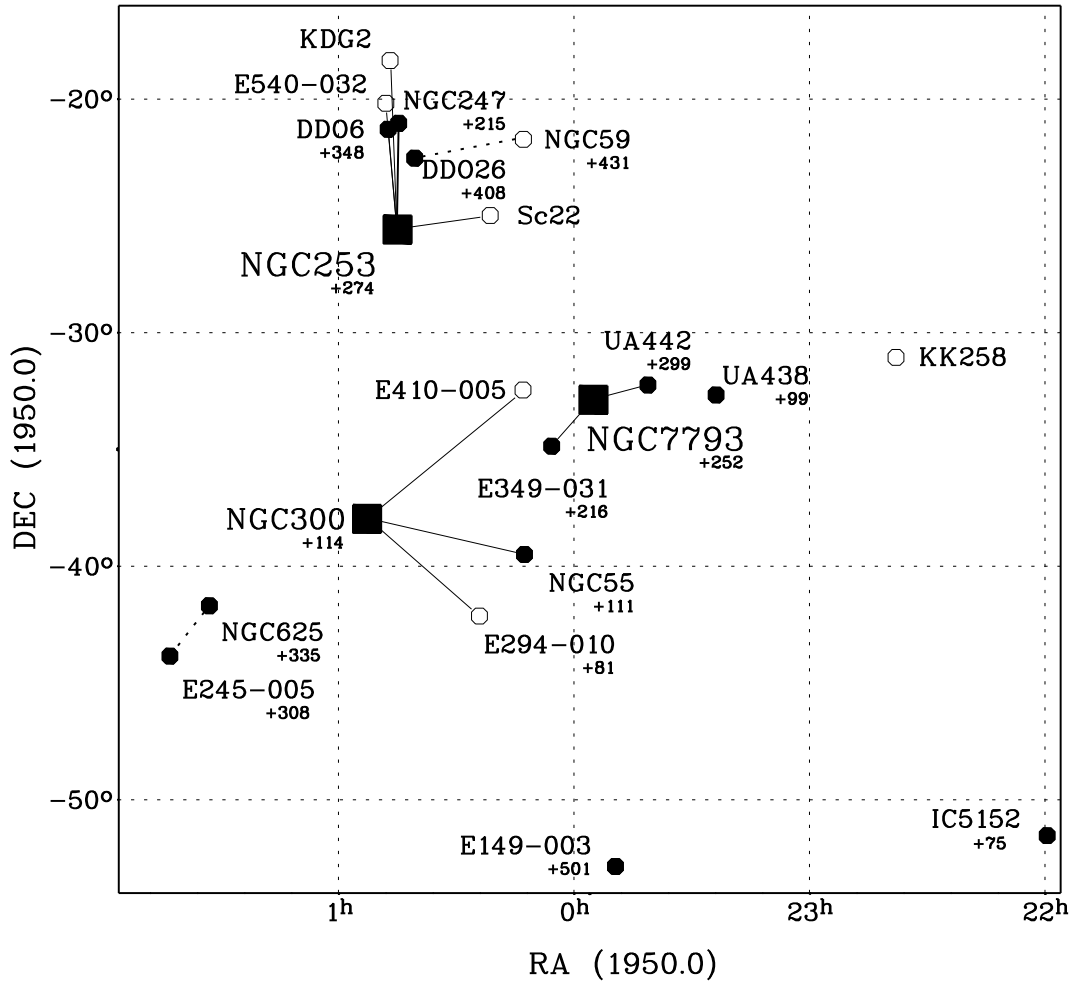


**Fig. 3.** Sky distribution of nearby galaxies in the direction of the Sculptor group. Filled and open circles indicate dwarf irregular and dwarf spheroidal galaxies, respectively. Large squares correspond to the most luminous galaxy in each group. Their probable companions are connected to the principal galaxies with straight lines. Radial velocities of the galaxies relative to the Local Group centroid are indicated by small numbers.



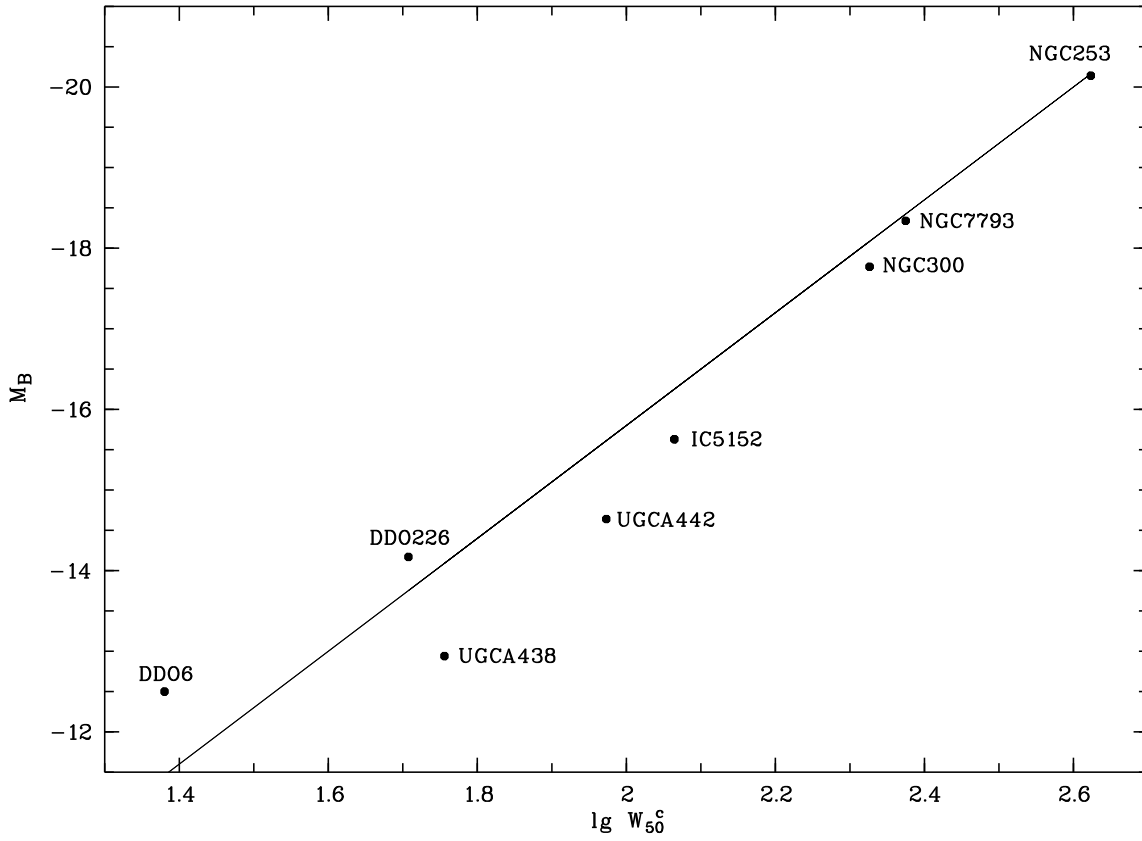


**Fig. 4.** Tully-Fisher relation for eight galaxies in Sculptor with accurate distances.

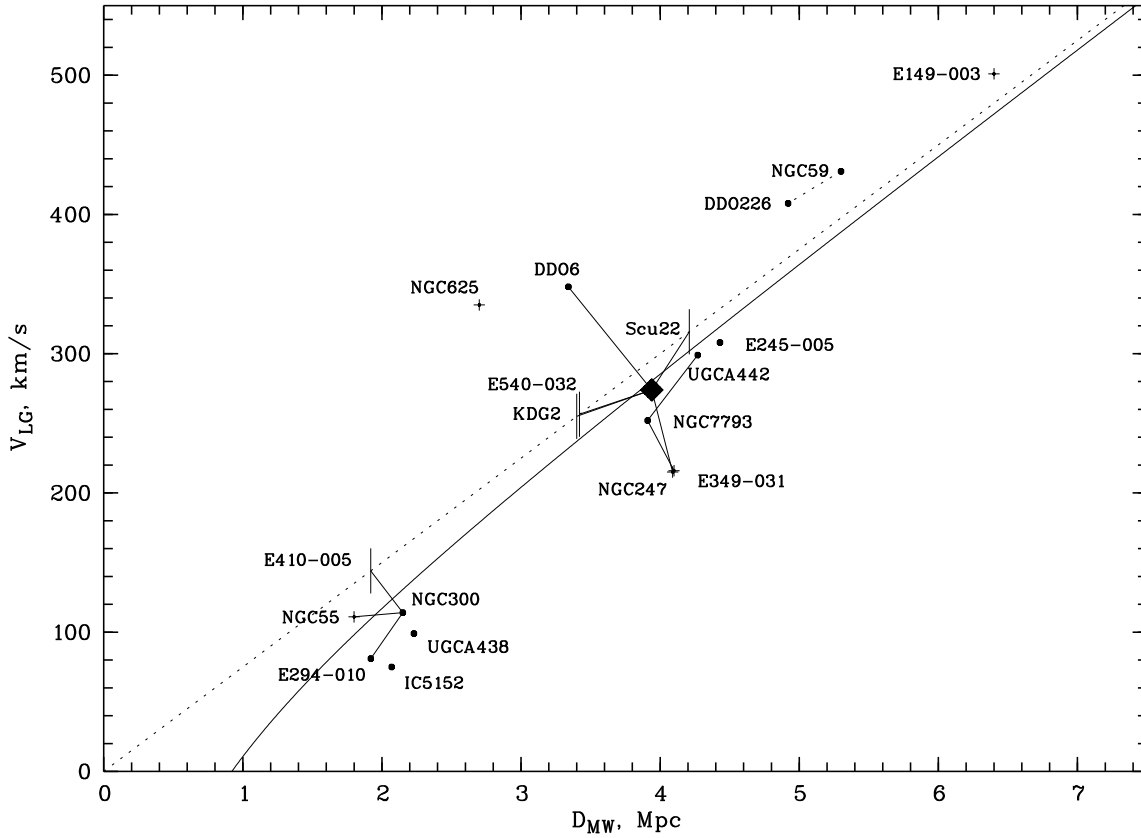


**Fig. 5.** Radial velocity – distance relation for 20 nearby galaxies in Sculptor. The galaxies with accurate distance estimates are shown as filled circles, and galaxies with T-F distances are shown as crosses. Four dSph galaxies without radial velocities are indicated by vertical bars. The brightest galaxy, NGC 253, is indicated by a square. The solid line corresponds to the Hubble relation with  $H = 75 \text{ km s}^{-1} \text{ Mpc}^{-1}$ , curved at small distances assuming a decelerating gravitational action of the Local Group with a total mass of  $1.3 \cdot 10^{12} M_{\odot}$ . Probable companions of the most luminous galaxies are connected with these by straight lines.

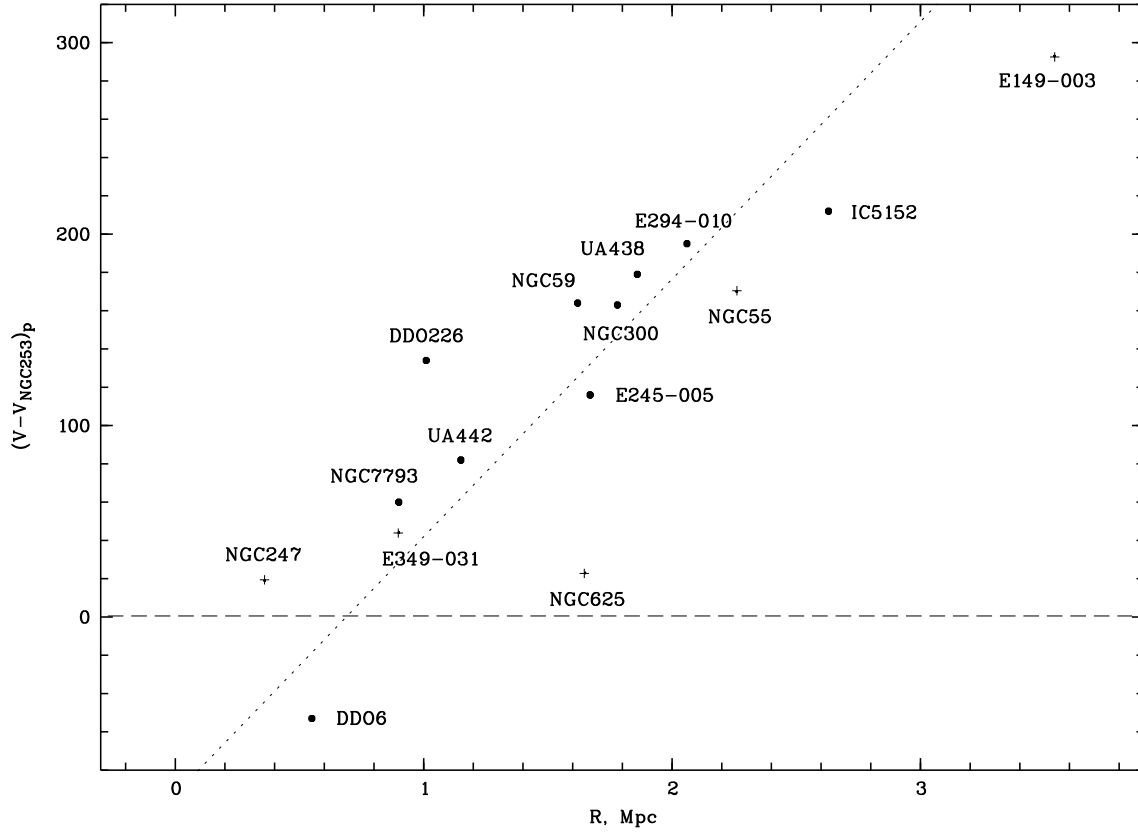


**Fig. 6.** The distribution of the radial velocity difference and the distance of nearby galaxies with respect to NGC 253. These data yield a radius of the zero-velocity surface of  $R_0 = 0.7$  Mpc.